Proc. Natl. Acad. Sci. USA
Vol. 88, pp. 1621–1625, March 1991
Neurobiology

Dissociation of object and spatial visual processing pathways in human extrastriate cortex

(regional cerebral blood flow/positron emission tomography)

JAMES V. HAXBY*†, CHERYL L. GRADY*, BARRY HORWITZ*, LESLIE G. UNGERLEIDER‡, MORTIMER MISHKIN‡, RICHARD E. CARSON§, PETER HERSCOVITCH§, MARK B. SCHAPIRO*, AND STANLEY I. RAPOPORT*

*Laboratory of Neurosciences, National Institute on Aging, ‡Laboratory of Neuropsychology, National Institute of Mental Health, and §Positron Emission Tomography Section, Department of Nuclear Medicine, National Institutes of Health, Bethesda, MD 20892

Contributed by Mortimer Mishkin, November 7, 1990

ABSTRACT **The existence and neuroanatomical locations of separate extrastriate visual pathways for object recognition and spatial localization were investigated in healthy young men. Regional cerebral blood flow was measured by positron emission tomography and bolus injections of $H_2{}^{15}O$, while subjects performed face matching, dot-location matching, or sensorimotor control tasks. Both visual matching tasks activated lateral occipital cortex. Face discrimination alone activated a region of occipitotemporal cortex that was anterior and inferior to the occipital area activated by both tasks. The spatial location task alone activated a region of lateral superior parietal cortex. Perisylvian and anterior temporal cortices were not activated by either task. These results demonstrate the existence of three functionally dissociable regions of human visual extrastriate cortex. The ventral and dorsal locations of the regions specialized for object recognition and spatial localization, respectively, suggest some homology between human and nonhuman primate extrastriate cortex, with displacement in human brain, possibly related to the evolution of phylogenetically newer cortical areas.**

In nonhuman primates, extrastriate visual cortical areas are broadly organized into two anatomically distinct and functionally specialized pathways: an occipitotemporal pathway for identifying objects and an occipitoparietal pathway for perceiving the spatial relations among objects (1–3). These pathways receive their inputs from cells in striate cortex with relays in prestriate cortex. The object vision pathway projects ventrally to inferior temporal cortices (areas TEO and TE) extending forward to the temporal pole. The spatial vision pathway projects dorsally to inferior parietal cortex (area PG). The existence of similar pathways in humans is suggested by the differential visual effects of focal occipitotemporal and occipitoparietal lesions in clinical cases (4–9), but the anatomical resolution afforded by studies that rely on accidents of nature is necessarily coarse. We therefore sought to delineate the object and spatial vision pathways in awake, healthy human subjects by measuring regional cerebral blood flow (rCBF) with positron emission tomography (PET) (10, 11) while the subjects performed selective visual tasks. Our results identify specific occipitotemporal and superior parietal regions associated with object and spatial visual processing, respectively, and a lateral occipital region associated with both visual functions.

METHODS

Subjects. Eleven young men participated in this study. All subjects were healthy, as established by physical examination, medical history, and routine laboratory tests. Mean subject age was 24.9 yr (SD = 4.6). All subjects gave written informed consent.

Visual Processing Tasks. rCBF was measured while subjects performed different visual match-to-sample tasks. Face matching was used to probe for object vision areas and dot-location matching was used for spatial vision areas (Fig. 1). The subject indicated which of two choice stimuli matched the simultaneously presented sample stimulus by pressing a button with his left or right thumb. To control for rCBF increases due to simple visual stimulation or thumb movement, rCBF also was measured during the performance of a sensorimotor control task, in which the subject pressed a button, alternately with the left and right thumbs, each time a control stimulus, three empty squares, was presented. Stimuli were presented on a rear projection screen that was placed at a 35° angle, relative to horizontal, and was 55 cm from the subject's eyes. The subject had to gaze downward to see the stimuli. The rest of the visual field was obscured by white drapes or was occupied by the inside of the tomograph ring. Stimulus presentation ended 500 msec after the subject made a response, allowing time for self-correction. Eye movements were not restricted. Subjects performed each task for a total of 5 min, beginning 1 min before the injection of the radioactive tracer.

PET. rCBF was measured six times in each subject with PET. The first and last rCBF scans were obtained while the subject performed the sensorimotor control task. Two rCBF scans were obtained for each visual processing task. The order of object and spatial vision scans was counterbalanced across subjects. Head movement was restricted with a thermoplastic mask, allowing pixel-by-pixel within-subject comparisons of rCBF during the various tasks.

Subjects received bolus injections of 30 mCi (1 Ci = 37 GBq) of $H_2{}^{15}O$ 1 min after beginning each task. The time course of regional brain radioactivity concentrations was measured with a Scanditronix PC1024-7B tomograph (Uppsala, Sweden) during the 4 min after the tracer reached the brain, simultaneously in seven parallel, cross-sectional planes with an in-plane resolution of 6 mm and an axial resolution of 11 mm. Planes were parallel to the inferior orbitomeatal (IOM) line and spaced 14 mm apart (center to center); 1.7–4.1 million counts were obtained for each image plane. Transmission scans were obtained in the same image planes as the emission scans and were used to correct for attenuation. Quantitative images of rCBF (ml per min per 100 g of brain) were produced by using the sampled arterial blood time activity curve and the weighted integration method (13). The two scans for each task were averaged by calculating mean rCBF for each pixel (each 4

The publication costs of this article were defrayed in part by page charge payment. This article must therefore be hereby marked "*advertisement*" in accordance with 18 U.S.C. §1734 solely to indicate this fact.

Abbreviations: PET, positron emission tomography; rCBF, regional cerebral blood flow; IOM, inferior orbitomeatal.
†To whom reprint requests should be addressed.

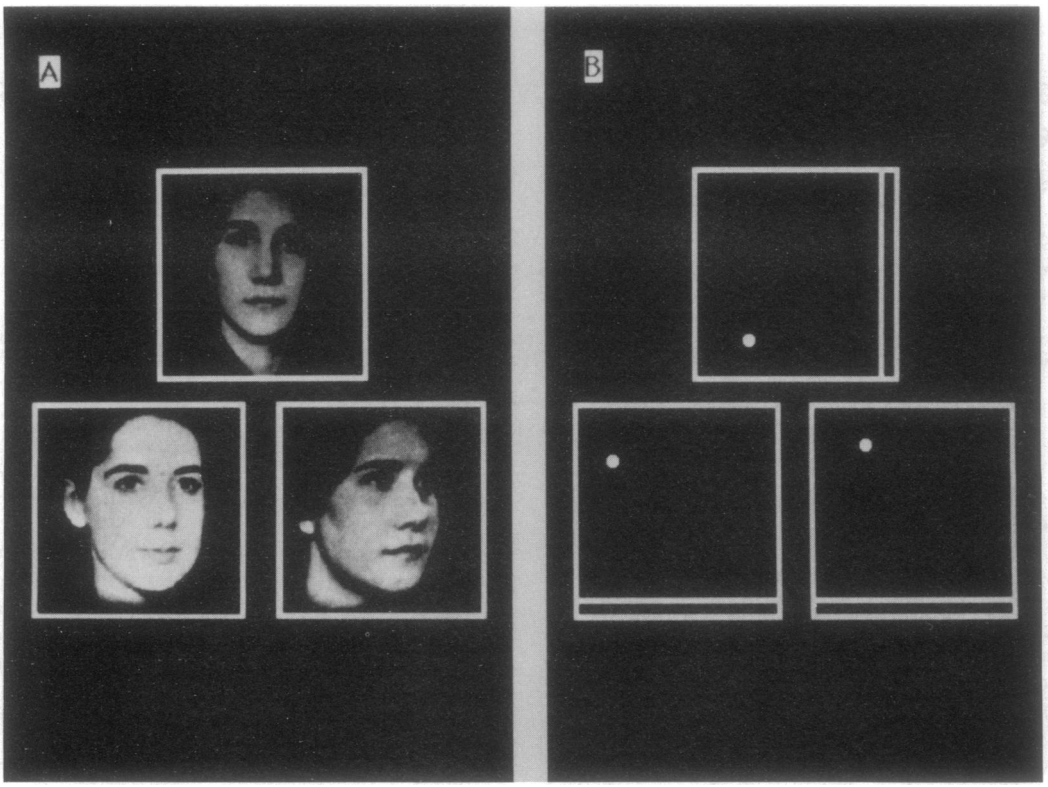

FIG. 1. (*A*) Item from the face discrimination task. The subject indicates which of the lower squares contains a picture of the same person shown in the upper square. The faces are from the Benton facial recognition test (12). (*B*) Item from the spatial vision task. The subject indicates which of the lower squares has the dot in the same location, relative to the double line, as the upper square.

mm^2). Mean rCBF values were then converted to percentages by dividing by whole brain CBF. CBF was calculated as the pixel-weighted average of whole brain regions of interest that were drawn on each image plane, using an automatic edge-finding routine to include all gray matter, white matter, and ventricles. Difference images that contrasted each visual processing task to the control task were constructed by subtracting control rCBF from stimulated rCBF for each pixel. A second set of difference images that directly contrasted rCBF during face matching to rCBF during dot-location matching was also constructed. The difference images were then smoothed with a Gaussian function, resulting in a final in-plane resolution of 9 mm.

Data Analysis. Two analyses were applied to these data. First, regions that demonstrated large rCBF increases in individual subjects were identified and their neuroanatomical locations were determined. Second, rCBF changes in these regions were quantified for statistical analysis. Analysis was restricted to the temporal, parietal, and occipital cortices.

Activated regions within an image plane were defined as ones containing at least 12 contiguous pixels (48 mm^2), demonstrating an increase in normalized rCBF over control values of at least 30%. This criterion was chosen as a conservative method to identify regions demonstrating rCBF increases that clearly exceeded statistical noise. Statistical noise in subtraction images was estimated by examining the distribution of pixel values in images with no major areas of activation. The mean SD of pixel values on subtraction images derived from four rCBF scans (mean visual processing rCBF − mean sensorimotor control rCBF) was 13%. A 30% increase, therefore, exceeded this estimate of statistical noise by >2 SD.

Activated regions were mapped onto the lateral or medial surface views of a standard brain from a brain atlas (14). Each image plane was matched to a horizontal section from the brain atlas based on neuroanatomical features discernible in the sensorimotor control rCBF image (15). This match determined the location of that image plane in the vertical dimension. Rostrocaudal location of a region with increased rCBF was determined by measuring the anterior and posterior limits of the region relative to the anterior and posterior limits of the brain. Regions were then mapped to the standard brain preserving proportional distances.

To quantify the normalized rCBF increases in the regions that were consistently activated during performance of the face or dot-location matching tasks, a procedure was developed that focused on local peak rCBF changes in individual subjects, thus accommodating individual differences in functional neuroanatomy, but did not yield inflated values due to statistical noise. Two statistically independent difference images were constructed for each condition, one contrasting the first runs of matching and control tasks and the other contrasting the second runs. Circular templates, 12 pixels (48 mm^2) in area, were placed on each scan in left and right lateral occipital cortex (40–50 mm above IOM), occipitotemporal cortex (30–35 mm above IOM), and superior parietal cortex (85–100 mm above IOM) and then moved, within the region of interest, until the maximum mean rCBF difference was located. Thus, the occipitotemporal template was always placed on a lower image than was the lateral occipital template, and also in a more anterior location, centered on average 3.4 cm (SD = 0.9 cm) anterior to the occipital pole as compared to 1.9 cm (SD = 0.9 cm). The locations of the templates were then transferred to the other difference image contrasting the same task conditions (visual matching − control) from different runs, and the mean normalized rCBF difference on that image was calculated and used as an unbiased estimate for statistical analysis. Thus, two estimates of rCBF change were obtained for each region, one from the template placed on the difference image from the first-run rCBF scans and the other from the template placed

on the difference image from the second-run rCBF scans. The means of these estimates were used for analysis.

RESULTS

Consistent differences were observed between the patterns of relative rCBF increases during object and spatial vision tasks, the former activating occipitotemporal and the latter activating superior parietal cortex. These differential activations are mapped for all subjects in Fig. 2, which is a composite of areas demonstrating activations in two or more subjects. The face-matching task caused rCBF increases in a broad region extending from the occipital pole to posterior temporal cortex in all subjects. The dot-location matching task caused rCBF increases in lateral occipital cortex in 8 of 11 subjects and rCBF increases in superior parietal cortex in 10 of 11 subjects. The lateral occipital area activated during spatial visual processing overlapped with the areas activated during face matching but tended to be closer to the occipitoparietal border and did not include the more anterior and inferior occipitotemporal region. Striate and extrastriate regions on the medial surface of the brain demonstrated less consistent activations that did not distinguish the two visual tasks. Many areas of temporal and parietal cortex were notably devoid of rCBF changes—namely, mid and anterior temporal cortex, as well as perisylvian cortex in the superior temporal gyrus and inferior parietal lobule.

A double dissociation between the visual functions of occipitotemporal and superior parietal cortex could be discerned in the individual data of 9 of the 11 subjects. Based on our conservative criteria for activated regions, these 9 individuals all demonstrated significant occipitotemporal rCBF activations during the face-matching task with either absent (n = 6) or less extensive (n = 3) activations of this region during dot-location matching, in conjunction with significant superior parietal rCBF activations during dot-location matching with absent (n = 6) or less extensive (n = 3) activations of this region during face matching. An additional subject showed only superior parietal activation during dot-location matching and only lateral occipital activation during face matching. The remaining subject demonstrated a clearly anomalous pattern, exhibiting both occipitotemporal and superior parietal activations during face matching and only right lateral occipital activation during dot-location matching.

Occipitotemporal activations during face matching and superior parietal activations during dot-location matching were usually bilateral. Of the 10 subjects with occipitotemporal activations during face matching, 8 had bilateral activations, 1 activated the left side only, and 1 activated the right side only. Of the 10 subjects with superior parietal activations during dot-location matching, 6 had bilateral activations, 2 activated the left side only, and 2 activated the right side only. In lateral occipital cortex, activation was observed during face matching in 10 subjects (7 bilateral, 2 on the left only, 1 on the right only) and during dot-location matching in 8 subjects (5 bilateral, 1 on the left side only, 2 on the right side only).

To visualize areas activated differentially by the two matching tasks, we constructed difference images that contrasted face matching and dot-location matching and identified regions (12 or more pixels in extent) demonstrating large differences

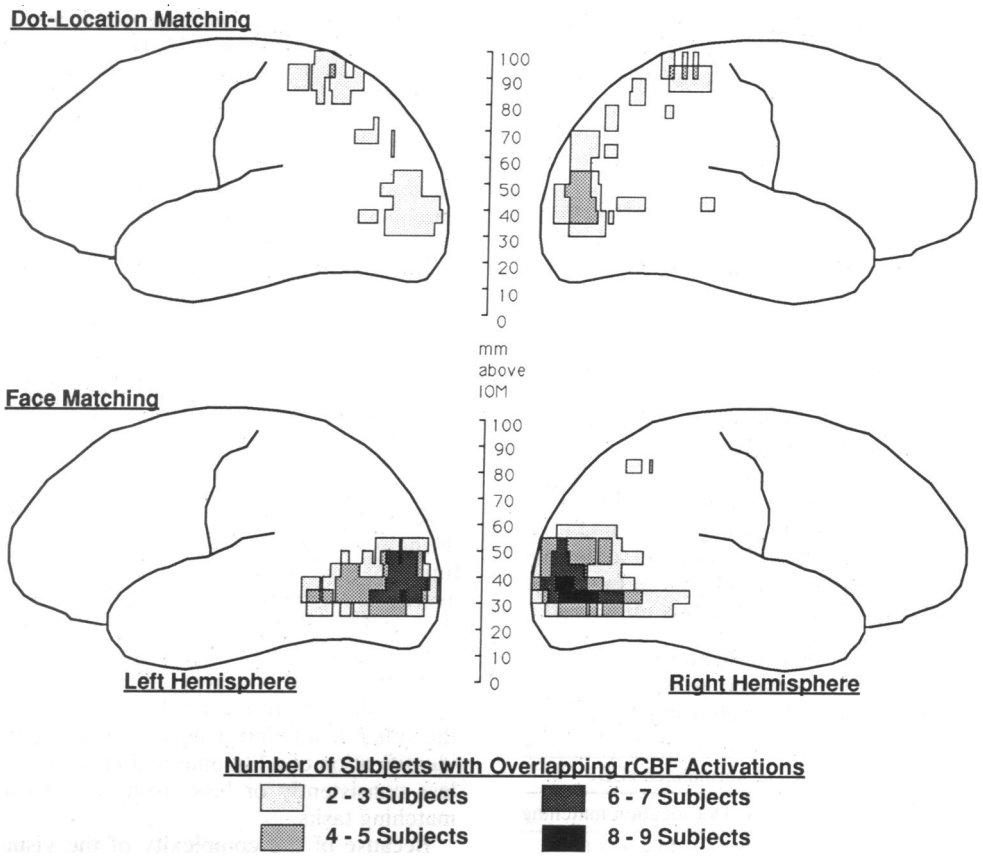

FIG. 2. Parietal, occipital, and temporal lobe regions in which two or more subjects demonstrated substantial increases in normalized rCBF during face matching or dot-location matching as compared to rCBF during a sensorimotor control task. Only regions with 12 contiguous pixels (48 mm^2), each demonstrating at least a 30% difference in normalized rCBF, were plotted. The number of subjects demonstrating rCBF increases in any specific location is indicated by shading. During dot-location matching, 8 of 11 subjects had lateral occipital rCBF increases and 10 of 11 subjects had superior parietal rCBF increases. During face matching, 10 of 11 subjects had lateral occipital rCBF increases and 10 of 11 subjects demonstrated occipitotemporal rCBF increases.

(30% or greater) using the same criterion for activated regions that were described above. Areas activated more by dot-location matching than by face matching in two or more subjects were always located in superior parietal cortex >85 mm above the IOM line. By contrast, areas activated more by face matching than by dot-location matching in two or more subjects were always in lateral occipital and occipitotemporal cortex between 25 and 55 mm above the IOM line. Examination of individual subjects' data again revealed that this double dissociation of effects was evident in 9 of the 11 subjects. No medial occipital areas were identified that were differentially activated by these visual tasks.

Quantification of the magnitudes of the rCBF increases in these regions by the methods described above (Table 1) revealed no significant differences between right- and left-hemisphere rCBF increases ($P > 0.05$). The face-matching task caused significant normalized rCBF increases in lateral occipital and occipitotemporal cortex but not in superior parietal cortex. By contrast, the dot-location matching task significantly increased normalized rCBF in lateral occipital and superior parietal cortex but not in occipitotemporal cortex. The difference in effect between normalized rCBF values during face matching and dot-location matching tasks in lateral occipital cortex was not significant ($t = 1.27$; $P > 0.2$), but the differences in the effects of the two tasks were significant in occipitotemporal and superior parietal cortex ($t = 2.61$ and $P < 0.05$; $t = 3.14$ and $P < 0.05$, respectively).

DISCUSSION

The results demonstrate three extrastriate visual-processing regions in the intact human brain involved in object and spatial vision. A lateral occipital, extrastriate region is involved in both visual functions. Still higher-order occipitotemporal and superior parietal visual areas are functionally specialized for object and spatial vision, respectively. This configuration indicates a bifurcation of visual processing streams in human cortex into dorsal and ventral pathways that may be homologous to the visual pathways described in nonhuman primates (Fig. 3).

The activations in these three regions were bilateral in most subjects, and it is likely that the unilateral activations noted in some subjects are due to a threshold effect stemming from the conservative criterion used to define activated regions. The quantitative analysis revealed no asymmetries of activations in any of these regions.

The locations of the activated regions were determined by orienting all image planes parallel to a line defined by skull landmarks (IOM) and by discerning neuroanatomical landmarks directly from the rCBF images (16). Others have found that the IOM line has a less consistent location relative to neuroanatomical structures than does another line defined by skull landmarks, that connecting the glabella and inion (17). Consequently, the error in localization may be somewhat larger than it would have been had we referenced the image planes to the glabellar–inion line. Despite this imprecision,

Table 1. Mean bilateral increases of normalized rCBF (percentage of whole brain CBF) in lateral occipital, occipitotemporal, and superior parietal regions during face matching and dot-location matching

	Increases of normalized rCBF	
	Face matching	Dot-location matching
Lateral occipital	16.6 ± 4.3*	10.4 ± 2.0†
Occipitotemporal	16.3 ± 4.6*	3.6 ± 2.9
Superior parietal	3.4 ± 2.0	12.9 ± 2.7†

All values are means ± SE. Significant rCBF increase is measured as difference from 0 by two-tailed t test.
*$P < 0.01$.
†$P < 0.001$.

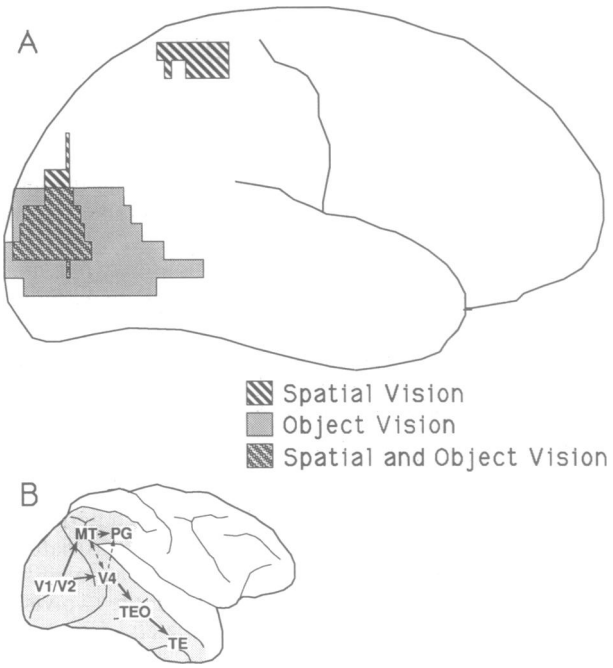

FIG. 3. Comparison of visual cortices in the macaque and extrastriate visual cortices in humans drawn in proportion to the relative sizes of the macaque and human brains. (*A*) A composite of posterior right and left cortical regions in which three or more subjects demonstrated increased normalized rCBF during face matching or dot-location matching as compared to rCBF during the sensorimotor control task. (*B*) A map of the major visual areas in macaque visual cortex and their interconnections, adapted from Desimone and Ungerleider (3). The results of the current study suggest homologies between the lateral occipital area activated by both tasks and lateral portions of area V4, the superior parietal area activated by the spatial task and area PG, and the occipitotemporal region activated by the object vision task and area TEO.

the double dissociation between areas activated by face matching and dot-location matching was clearly discernible, and the regions activated in individual subjects were assigned to locations that either overlapped or lay very close to those of other subjects. Moreover, the regions we have identified are all quite large and separated from one another by distances that are likely to be greater than the errors of measurement. The uncertainty of our methods of localization, however, has led us to assign these three visual areas to relatively broad areas of cortex, rather than to specific foci within individual gyri or sulci.

The pattern of regional rCBF activations during visual processing that we have described was clearly discernible in the individual data of 9 of 11 subjects. Thus, the evidence for functional specialization does not depend on intersubject averaging methods, which greatly increase the sensitivity of PET–rCBF techniques but are not designed to detect individual patterns (18). Restricting the analysis to data of individual subjects allowed an examination of the consistency of these patterns of rCBF increases across subjects. On the other hand, intersubject averaging may have allowed identification of additional regions that are significantly, but less consistently or less strongly, activated by the visual matching tasks.

Because of the complexity of the visual stimuli and the difficulty of matching them without eye movements, the subjects were not required to maintain fixations. Consequently, some of the increases in rCBF during visual matching over the levels seen during the control task may be attributable to differences in eye movements. Eye movement differences are a less likely explanation for the rCBF differ-

ences associated with the face-matching and dot-location matching tasks, both of which required comparisons among complex visual stimuli presented in the same three locations.

The lateral occipital region shared by both pathways lies in or near Brodmann area 19 and may correspond to visual area V4 (3, 19, 20). In the macaque, area V4 projects mainly to ventral extrastriate regions TEO and TE but also has projections to dorsal extrastriate regions MT and PG (3). Lueck *et al.* (21) have suggested that human area V4 lies in the lingual and fusiform gyri in inferior medial occipital cortex, based on rCBF studies of passive perception of color montages. Human rCBF studies of selective attention to color differences, however, have demonstrated activation in both medial and lateral occipital extrastriate cortices (22), suggesting that human V4 may extend from lateral to inferior to medial occipital cortex, as it does in the macaque (3, 20). In the present study, we did not find consistent rCBF increases in inferior medial occipital cortex during either task, perhaps because the stimuli were limited to black and white.

The bilateral occipitotemporal regions activated by face matching appear to lie in or near Brodmann area 37 and may correspond to area TEO in the macaque (3, 19). According to the present data, however, this area in humans is located more posteriorly than it is in the monkey. Mid and anterior temporal regions were not activated by face matching. Consequently, we have not identified any homologue for area TE, the next, more rostral cortical area in the ventral visual pathway in the macaque. Face discrimination might be expected to stimulate posterior regions more than anterior regions. In the monkey, lesions in the occipitotemporal junction of the object vision pathway (areas V4 and TEO) tend to have a greater effect on visual pattern discrimination than do lesions placed more anteriorly (area TE), whereas the anterior lesions have the greater effect on visual object recognition memory (23, 24). Studies of face perception in patients with surgical lesions suggest that there may be a similar functional distinction between occipitotemporal and anterior temporal regions in humans (25).

rCBF studies of word processing have shown that silent word reading also activates a region in or near area 37 in occipitotemporal cortex (26, 27). Selective attention to small differences in the shapes of rectangles (22), on the other hand, has been associated with increased rCBF in the lingual and fusiform gyri and in the superior temporal sulcus, not in area 37. These results suggest the possibility that area 37 is specialized for processing complex visual stimuli such as faces and words, whereas the processing of simpler visual shapes may be performed by other visual areas.

The spatial vision region we identified lies in the superior parietal lobule bilaterally. In the macaque, the region specialized for spatial vision, area PG or Brodmann area 7, is located in the inferior parietal lobule. Our findings suggest that the human homologue of this area is also area 7, which has been displaced to the superior parietal lobule. Human inferior parietal regions 39 and 40 have an architectonic structure that suggests they are phylogenetically new, and they apparently do not perform visual functions analogous to those performed in macaque inferior parietal cortex. Based on a study of patients with focal brain lesions, Posner *et al.* (28) concluded that the superior parietal lobule was more involved than the inferior parietal lobule in another spatial vision operation—namely, the ability to disengage and shift the spatial focus of visual attention.

These results suggest some homology between humans and nonhuman primates in the organization of cortical visual systems into "what" and "where" processing streams, with displacement in the locations of these systems due to the development of phylogenetically newer cortical areas. This functional division may have ramifications that extend beyond perceptual processing to visual functions that cannot be studied so easily in nonhuman primates, such as mental imagery (29–31), and to functions that humans do not share with nonhuman primates, such as language (32).

1. Ungerleider, L. G. & Mishkin, M. (1982) in *Analysis of Visual Behavior*, eds. Ingle, D. J., Goodale, M. A. & Mansfield, R. J. W. (MIT Press, Boston), pp. 549–586.
2. Mishkin, M., Ungerleider, L. G. & Macko, K. A. (1983) *Trends Neurosci.* **6**, 414–417.
3. Desimone, R. & Ungerleider, L. G. (1990) in *Handbook of Neuropsychology*, eds. Boller, F. & Grafman, J. (Elsevier, Amsterdam), Vol. 2, pp. 267–299.
4. Newcombe, F. & Russell, W. R. (1969) *J. Neurol. Neurosurg. Psychiatry* **32**, 73–81.
5. Ratcliff, G. & Davies-Jones, G. A. B. (1972) *Brain* **95**, 49–60.
6. Ratcliff, G. & Newcombe, F. (1973) *J. Neurol. Neurosurg. Psychiatry* **36**, 448–454.
7. Newcombe, F., Ratcliff, G. & Damasio, H. (1987) *Neuropsychologia* **25**, 149–161.
8. Damasio, A. R. & Benton, A. L. (1979) *Neurology* **29**, 170–178.
9. Damasio, A. R., Damasio, H. & Van Hoesen, G. W. (1982) *Neurology* **32**, 331–341.
10. Fox, P. T., Mintun, M. A., Raichle, M. E., Miezin, F. M., Allman, J. M. & Van Essen, D. C. (1986) *Nature (London)* **323**, 806–809.
11. Fox, P. T., Miezin, F. M., Allman, J. M., Van Essen, D. C. & Raichle, M. E. (1987) *J. Neurosci.* **7**, 913–922.
12. Benton, A. L. & Van Allen, M. W. (1973) *Test of Facial Recognition*, Publication No. 287, Neurosensory Center (Univ. Iowa, Ames, IA).
13. Alpert, N. M., Eriksson, L., Chang, J., Bergstrom, M., Litton, J. E., Coreia, J. A., Bohm, C., Ackerman, R. H. & Taveras, J. M. (1984) *J. Cereb. Blood Flow Metab.* **4**, 28–34.
14. Eycleshymer, A. C. & Schoemaker, D. M. (1911) *A Cross-Section Anatomy* (Appleton, New York).
15. Rumsey, J. M., Duara, R., Grady, C., Rapoport, J. L., Margolin, R. A., Rapoport, S. I. & Cutler, N. R. (1985) *Arch. Gen. Psychiatry* **42**, 448–455.
16. Friston, K. J., Passingham, R. E., Nutt, J. G., Heather, J. D., Sawle, G. V. & Frackowiak, R. S. J. (1989) *J. Cereb. Blood Flow Metab.* **9**, 690–695.
17. Fox, P. T., Perlmutter, J. S. & Raichle, M. E. (1985) *J. Comput. Assisted Tomogr.* **9**, 141–153.
18. Fox, P. T., Mintun, M. A., Reiman, E. M. & Raichle, M. E. (1988) *J. Cereb. Blood Flow Metab.* **8**, 642–653.
19. Damasio, H. & Damasio, A. R. (1989) *Lesion Analysis in Neuropsychology* (Oxford Univ. Press, New York).
20. Gattass, R., Sousa, A. P. B. & Gross, C. G. (1988) *J. Neurosci.* **8**, 1831–1856.
21. Lueck, C. J., Zeki, S., Friston, K. J., Deiber, M.-P., Cope, P., Cunningham, V. J., Lammertsma, A. A., Kennard, C. & Frackowiak, R. S. J. (1989) *Nature (London)* **340**, 386–389.
22. Corbetta, M., Miezin, F. M., Dobmeyer, S., Shulman, G. L. & Petersen, S. E. (1990) *Science* **248**, 1556–1559.
23. Iwai, E. & Mishkin, M. (1968) in *Neurophysiological Basis of Learning and Behavior*, eds. Yoshii, N. & Buchwald, N. A. (Osaka Univ. Press, Osaka), pp. 1–8.
24. Cowey, A. & Gross, C. G. (1970) *Exp. Brain Res.* **11**, 128–144.
25. Milner, B. (1980) in *Nerve Cells, Transmitters and Behaviour*, ed. Levi-Montalcini, R. (Pontificia Academia Scientarium, Vatican City), pp. 601–625.
26. Petersen, S. E., Fox, P. T., Posner, M. I., Mintun, M. & Raichle, M. E. (1988) *Nature (London)* **331**, 585–589.
27. Petersen, S. E., Fox, P. T., Posner, M. I., Mintun, M. & Raichle, M. E. (1989) *J. Cognit. Neurosci.* **1**, 153–170.
28. Posner, M. I., Walker, J. A., Friedrich, F. J. & Rafal, R. D. (1984) *J. Neurosci.* **4**, 1863–1874.
29. Roland, P. E. & Friberg, L. (1985) *J. Neurophysiol.* **53**, 1219–1243.
30. Roland, P. E. & Widen, L. (1988) in *Functional Brain Imaging*, eds. Pfurtscheller, G. & Lopes da Silva, F. H. (Hans Huber, Toronto), pp. 213–228.
31. Farah, M., Hammond, K., Levine, D. & Calvanio, R. (1988) *Cognit. Psychol.* **20**, 439–462.
32. Jackendoff, R. & Landau, B. (1991) in *Bridges Between Psychology and Linguistics: A Swarthmore Festschrift for Lila Gleitman*, eds. Napoli, D. J. & Kegl, J. (Erlbaum, New York), in press.